

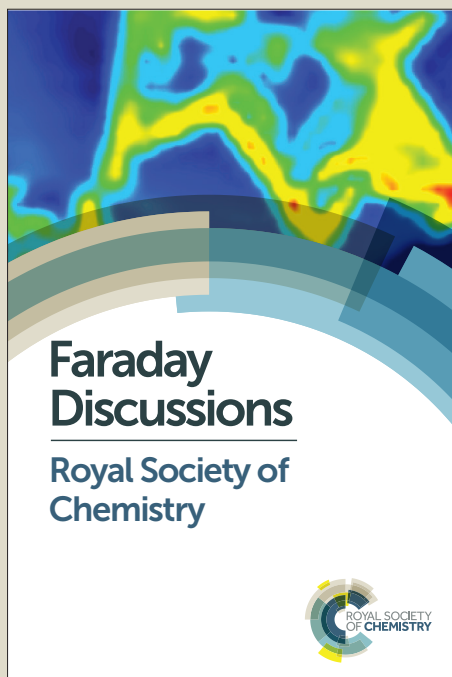
Faraday Discussions

Accepted Manuscript



This manuscript will be presented and discussed at a forthcoming Faraday Discussion meeting. All delegates can contribute to the discussion which will be included in the final volume.

Register now to attend! Full details of all upcoming meetings: <http://rsc.li/fd-upcoming-meetings>



This is an *Accepted Manuscript*, which has been through the Royal Society of Chemistry peer review process and has been accepted for publication.

Accepted Manuscripts are published online shortly after acceptance, before technical editing, formatting and proof reading. Using this free service, authors can make their results available to the community, in citable form, before we publish the edited article. We will replace this *Accepted Manuscript* with the edited and formatted *Advance Article* as soon as it is available.

You can find more information about *Accepted Manuscripts* in the [Information for Authors](#).

Please note that technical editing may introduce minor changes to the text and/or graphics, which may alter content. The journal's standard [Terms & Conditions](#) and the [Ethical guidelines](#) still apply. In no event shall the Royal Society of Chemistry be held responsible for any errors or omissions in this *Accepted Manuscript* or any consequences arising from the use of any information it contains.

Organic semiconductor distributed feedback laser pixels for lab-on-a-chip applications fabricated by laser-assisted replication

Xin Liu,^{ab} Stephan Prinz,^{a+} Heino Besser,^{cd} Wilhelm Pfleging,^{cd}
5 Markus Wissmann,^{bd} Christoph Vannahme,^{ba++} Markus
Guttmann,^{bd} Timo Mappes,^{b+++} Sebastian Köber,^{be} Christian Koos,^{be}
and Uli Lemmer^{*ab}

DOI: 10.1039/b000000x [DO NOT ALTER/DELETE THIS TEXT]

The integration of organic semiconductor distributed feedback (DFB) laser
10 sources into all-polymer chips is promising for biomedical or chemical
analysis. However, the fabrication of DFB corrugations is often expensive
and time-consuming. Here, we apply the method of laser-assisted
replication using a near-infrared diode laser beam to efficiently fabricate
15 inexpensive poly(methyl methacrylate) (PMMA) chips with spatially
localized organic DFB laser pixels. This time-saving fabrication process
enables a predefined positioning of nanoscale corrugations on chip and a
simultaneous generation of nanoscale gratings for organic edge-emitting
laser pixels next to microscale waveguide structures. A single chip of
30 mm × 30 mm size can be processed within 5 min. Laser-assisted
20 replication allows for a subsequent addition of further nanostructures
without negative impact on existing photonic components. The minimum
replication area can be defined as small as the diode laser beam focus spot
size. To complete the fabrication process, we encapsulate the chip in
PMMA using laser transmission welding.

25 1 Introduction

Organic semiconductor distributed feedback (DFB) lasers are of particular interest
as tunable laser emitters covering the whole visible spectral range.¹⁻⁵ Enabled by the
efficient conversion in their active material, low threshold organic semiconductor
lasers allow for free space and integrated excitation sources in spectroscopic
30 investigations.⁶⁻⁹ Particularly, the use of miniaturized laser pixels in all-polymer lab-
on-a-chip (LOC) systems combined with passive photonic components is promising
for bio-medical point of care analysis.¹⁰⁻¹⁴ In order to realize laser pixels,

^a Light Technology Institute (LTI), Karlsruhe Institute of Technology, 76131 Karlsruhe, Germany

^b Institute of Microstructure Technology (IMT), Karlsruhe Institute of Technology, 76344
Eggenstein-Leopoldshafen, Germany

^c Institute for Applied Materials - Applied Materials Physics (IAM-AWP), Karlsruhe Institute of
Technology, 76344 Eggenstein-Leopoldshafen, Germany

^d Karlsruhe Nano Micro Facility, Hermann-von-Helmholtz-Platz 1, 76344 Eggenstein-
Leopoldshafen, Germany

^e Institute of Photonics and Quantum Electronics (IPQ), Karlsruhe Institute of Technology, 76131
Karlsruhe, Germany

+ currently with TRUMPF Scientific Lasers GmbH + Co. KG, 85774 Unterföhring-München,
Germany

++ currently with DTU Nanotech, Technical University of Denmark, 2800 Kgs. Lyngby, Denmark

+++ currently with Carl Zeiss AG, Corporate Research and Technology, 07745 Jena, Germany

* E-mail: uli.lemmer@kit.edu

technologies for local definition of the active material and for the laterally controlled fabrication of DFB-structures have to be developed.

In terms of the gain materials, small molecules such as tris(8-hydroxyquinoline) aluminum (Alq₃) doped with the laser dye 4-(dicyanomethylene)-2-methyl-6-(*p*-dimethylaminostyryl)-4*H*-pyran (DCM) are competing with conjugated polymers. The former class of materials can be evaporated locally using shadow masking and can thus be combined with predefined grating structures. On the other hand, conjugated polymers can be processed by inexpensive solution-based techniques such as spin coating, dip-coating and doctor blading. These methods, however, result in an organic semiconductor layer covering the whole substrate. A lateral control can be achieved using printing techniques. A particularly interesting approach is the use of ink-jet printing. Ink-jet printing has already been successfully applied to the fabrication of various organic electronic devices, such as organic transistors^{15,16} organic solar cells^{17,18} and organic light-emitting diodes.^{19,20} We have recently successfully fabricated organic semiconductor distributed feedback laser pixels by ink-jet printing the active layer from a conjugated polymer solution. Utilizing an optimized mixture of high-boiling and low-boiling solvents for dissolving the polymer, the ink-jet-printed film profile is optimized, thus creating uniformly emitting organic lasers. Such devices show lasing thresholds as low as 76 nJ/pulse and a spectrally homogeneous laser emission over large areas.²¹

The laterally controlled fabrication of DFB-gratings for organic semiconductor lasers has only been addressed so far by using nanograting transfer to transfer a the gratings onto a homogeneous gain material layer²² and a rather complex approach using direct electron beam lithography (EBL) on conjugated polymers.²³ On the other hand, various substrate scale techniques such as laser interference lithography (LIL)²⁴ and nanoimprint lithography (NIL)²⁵ are available to achieve a low-cost fabrication of high-quality DFB corrugation nanostructures on an LOC platform. Among them, NIL promises a mass-production of extremely fine structures with feature sizes down to 10 nm.²⁶ The resolution of NIL can be further improved by the fabrication of a rigid mold with sub-10 nm features.²⁵ Nowadays, two main subjects of NIL are frequently used in fabrication of DFB corrugations for organic semiconductor laser applications: thermal nanoimprint lithography (TNIL, also known as hot embossing) and UV-assisted nanoimprint lithography (UV-NIL).²⁷⁻³⁰ UV-NIL can be an option to fabricate localized DFB corrugations without negative effects on existing structures, but it is mandatory to use special photoactive materials in the process. This limitation results in a narrow application field in fabrication of LOC systems. TNIL is advantageous for parallel replication of all structures from a master stamp onto a common polymer substrate. Nevertheless, it has three major drawbacks: First is the difficulty in fabrication of predefined partial structures from a rigid master stamp with structures for different purposes. Secondly, the large-area heating can be detrimental for existing LOC passive photonic elements and microfluidic channels. The third issue is long heating and cooling time.

These limitations of TNIL can be overcome using a near-infrared high-power diode laser beam.^{31,32} In this work, we demonstrate a novel laser-assisted replication to fabricate localized surface-emitting (2nd order) and edge-emitting (1st order) organic distributed DFB laser pixels on a poly(methyl methacrylate) (PMMA) substrate. Our technique allows for a fast replication with standard TNIL materials due to the localized heating. Not only is the process time reduced, the localized

heating also provides the unique benefit to replicate only parts of the existing structures on a master stamp. Additionally, since only the defined areas are to be heated, it allows for a subsequent additive fabrication of DFB corrugations while all other areas are retained. The minimum localized replication area and the influence of process parameters on corrugation quality are investigated. A functional LOC is finished after encapsulation via laser transmission welding protecting the device from air and water.³³⁻³⁵

2 Fabrication process

In laser-assisted replication, a rigid mold, e.g., a silicon master stamp is pressed under a polymer substrate and the contact area is subsequently heated up by a near-infrared laser beam from above, as shown in Fig. 1(a). Due to heat conduction the temperature of the polymer material which is in direct contact with the master stamp increases. When the temperature exceeds the polymer glass transition temperature, the nanostructures on the rigid mold are replicated into the polymer substrate. After cooling down, the polymer substrate is detached from the rigid mold while the nanostructures are preserved.

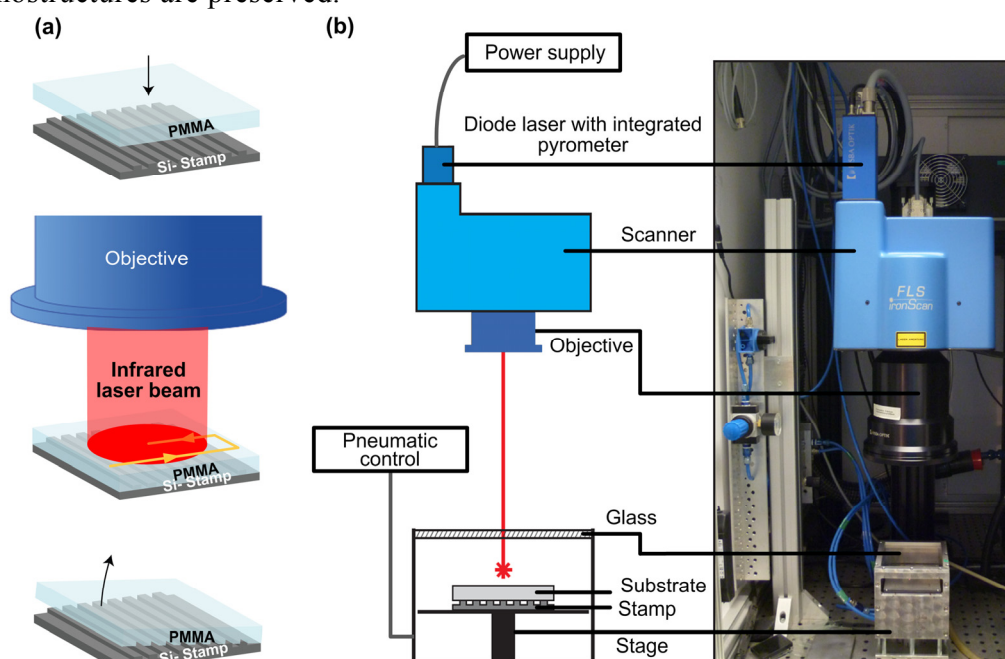


Fig. 1 (a) Scheme of the laser-assisted replication process: positioning of the PMMA substrate on a silicon master stamp (top), execution of the replication (middle) and detachment of the sample (bottom). (b) Schematic illustration (left) and photograph (right) of the applied laser system.

To perform the experiments, a high-power diode laser system (Fisba Optik, FLS Iron High Power Diode) with an emission wavelength of 940 nm and a maximal power of 50 W is used. As shown in Fig. 1(b), the diode laser and a pyrometer, which provides an in-situ monitoring of the temperature at the laser focus plane, are integrated within the laser scanner unit. The PMMA substrate and the silicon master stamp are fixed in a pneumatic stage, applying a constant pressure. There are two basic operation modes of the system: constant laser power or constant heating temperature. In our case, the temperature regulation is chosen in order to achieve a homogeneous temperature distribution at the contact surface. Utilizing an F-Theta objective lens (Fisba Optik) with a focal length of 163 mm, the size of the elliptical laser focus spot on the work plane is 0.55 mm × 0.7 mm. Attributed to the applied

scanner system, the maximum laser processing area can reach $100\text{ mm} \times 100\text{ mm}$.

Before replication, a silicon master stamp was fabricated. Via electron beam lithography and reactive ion etching (RIE), the DFB corrugations with grating periods ranging from 195 nm to 450 nm, a height of $\sim 120\text{ nm}$ and a duty cycle of 75% were generated. Via aligned UV-lithography and subsequent RIE on the same wafer, basins for the DFB lasers with a height of $1.2\text{ }\mu\text{m}$ were finished. A thin anti-adhesion layer was then deposited on the wafer to facilitate the polymer substrate detachment.¹³

For the replication process, a 2 mm-thick PMMA substrate (Evonik, Plexiglas® XT) with a size of $30\text{ mm} \times 30\text{ mm}$ was positioned on selected corrugations of the silicon master stamp. The following process parameters resulted in highest quality replication: a heating temperature of $T = 180\text{ }^\circ\text{C}$, a laser scan velocity of $v = 40\text{ mm/s}$, a clamping pressure of $p = 0.1\text{ MPa}$ and a hatch distance (offset between two neighboring laser tracks) of $\Delta x = 300\text{ }\mu\text{m}$. To achieve a homogenous replication, each substrate was treated twice by the laser beam: first perpendicular to grating orientation, as shown in Fig. 1(a), second parallel to the grating orientation. The replication process took about 5 min for the replication of an area of $40\text{ mm} \times 40\text{ mm}$. After replication, the clamping pressure was released. The PMMA substrate was cooled down with a nitrogen spray gun and separated from the silicon master stamp. Figure 2(a) and 2(b) show a microscope image and a scanning electron microscope image on PMMA of a grating with period of $\Lambda = 400\text{ nm}$. The grating structures fabricated via laser-assisted replication shows a high fidelity over the whole molding area. The replicated quality was similar to thermal nanoimprint lithography, as shown in Fig. 2(c). However, the laser-assisted replication process took a much shorter time compared to the 45 min-long TNIL process. The Alq_3 doped with the laser dye DCM has been chosen as the active material. It forms a very efficient Foerster energy transfer system and exhibits an excellent long-term stability. Evaporating 250 nm Alq_3 doped with 2.8 wt.% DCM onto the defined grating fields finally yielded the organic DFB laser pixels. The used stencil shadow mask was fabricated by UV-lithography and nickel electroplating.¹⁴

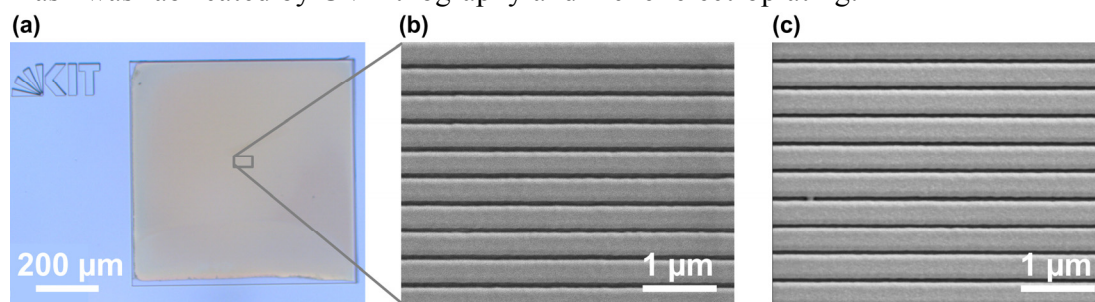


Fig. 2 (a) Microscope image of a one-dimensional PMMA DFB grating with a period of $\Lambda = 400\text{ nm}$ fabricated by laser-assisted replication. (b) Scanning electron microscope image of the grating structures fabricated by laser-assisted replication. For comparison (c) shows a scanning electron microscope image of the $\Lambda = 400\text{ nm}$ grating structures fabricated by thermal nanoimprint lithography (IMT-KIT, WUM) using the same silicon master stamp as for (b). A temperature of $180\text{ }^\circ\text{C}$ and a pressure of 1.85 MPa were applied for 15 min. The total TNIL process lasted for $\sim 45\text{ min}$.

3 DFB laser characterization

For optical characterization, the fabricated surface-emitting organic DFB lasers were excited by a diode-pumped, actively Q-switched frequency tripled neodymium:yttrium-orthovanadate (Nd:YVO_4) laser (Advanced Optical Technology

Ltd., AOT-YVO-20QSP) with a wavelength of 355 nm. The pump pulse energy was adjusted with a variable neutral density filter and measured with a calibrated gallium arsenide phosphide photodiode connected to an oscilloscope (Tektronix, TDS2024C). The sample was kept in a vacuum chamber ($< 5 \times 10^{-3}$ Pa) to protect the active material from photooxidation. The chamber can be shifted in the plane perpendicular to the excitation beam using an automated precision stage. This allows for a spectrally and spatially resolved characterization of the samples. A focusing lens was used to adjust the excitation spot size. Emission from the sample was collected using the focusing lens for the pump beam, then directed through a dichroic mirror and coupled into a multimode optical fiber. Further on, the laser spectra were analyzed using a spectrograph (Acton Research Corporation, SpectraPro 300i, variable grating) connected to an intensified charge-coupled device camera (Princeton Research, PiMax 512). The pump spot showed a slightly elliptical shape with a size of $30 \mu\text{m} \times 40 \mu\text{m}$ on the sample.

Figure 3(a) shows the color-encoded spatially resolved lasing wavelength from a PMMA chip containing 9 laser pixels with individual lateral dimension of $500 \mu\text{m} \times 500 \mu\text{m}$ and an interspacing of $500 \mu\text{m}$. The grating period of DFB corrugations varies from 370 nm to 450 nm in steps of 10 nm from the outermost left pixel to the outermost right one. The chip was probed with a resolution of $100 \mu\text{m}$. The laser emission wavelength did not show any deviation on the area of a single laser pixel within the spectral resolution of our setup (approximately 0.5 nm). This indicates a very uniform replication of nanogratings in PMMA. The corresponding laser emission spectra and the laser threshold values for TE_0 -modes are shown in Fig. 3(b) and 3(c). The higher laser threshold from the laser pixel with grating period of 450 nm is attributed to the lower gain coefficient at the emission wavelength of 712.5 nm.

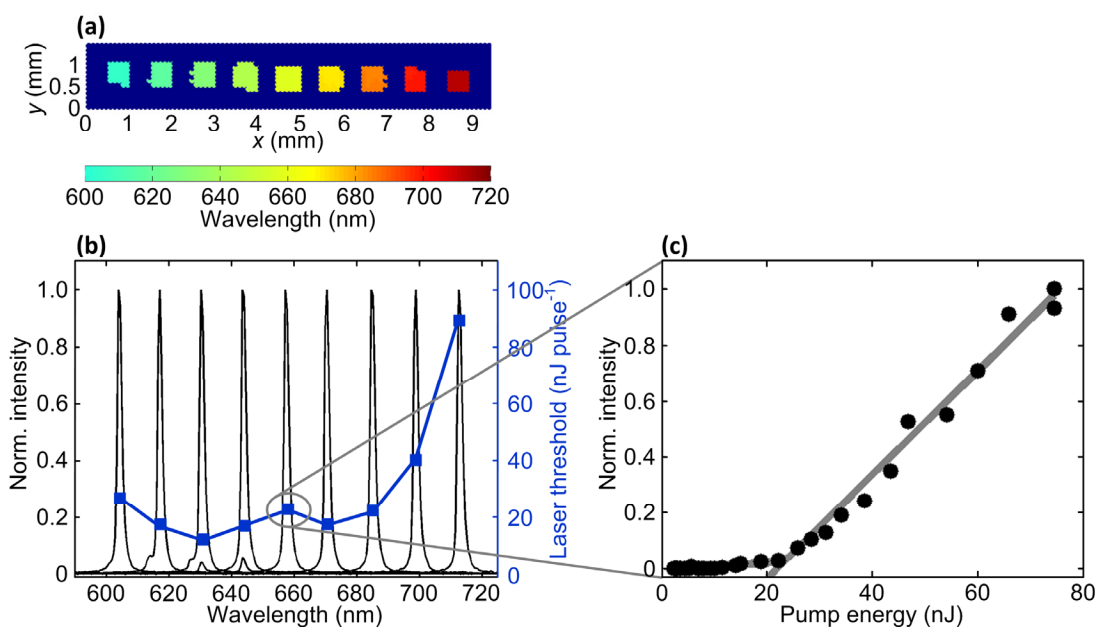


Fig. 3 (a) Color-encoded Spatially resolved laser wavelengths of fabricated organic DFB laser pixels with grating periods from 370 nm (left) to 450 nm (right) in steps of 10 nm. (b) Laser spectra and TE_0 -mode laser threshold corresponding to the grating distribution. For some gratings the onset of the TM_0 -mode can also be seen as very small peaks. (c) Input-output characteristic of a laser pixel with grating period of $\Lambda = 410$ nm and a laser emission at $\lambda = 657.5$ nm.

For being suitable for LOC spectroscopic applications, the organic semiconductor lasers are usually based on first-order DFB gratings for emission light in chip plane

only. By introducing a waveguide onto the chip, the first-order organic laser emission can be efficiently coupled and guided to the analyte sites. PMMA chips with via deep ultraviolet (DUV) induced waveguides have been fabricated previously.^{11,13} In this work, we fabricated the active grating and waveguides altogether via laser-assisted replication and evaporated Alq₃:DCM on both of them to build coupled edge-emitting organic laser on chip. This novel configuration allows for a one-step fabrication of laser and waveguide without mix-and-match pattern-related defects.³⁶ Besides, direct connection between laser and waveguide made from the same active material will facilitate an optimum coupling efficiency.

Different gratings with lateral dimensions of 500 μm, interconnected by 300 μm-wide waveguide structures perpendicular to the grating orientation were simultaneously fabricated in 1.2 μm-deep basins on PMMA chip. The grating periods for first-order organic DFB laser were chosen to be $\Lambda = 195$ nm, $\Lambda = 200$ nm, and $\Lambda = 205$ nm, as marked in Fig. 4(a). A 250 nm-thick layer of Alq₃:DCM was evaporated on the defined grating and waveguide, thus allowing for an optimum light coupling.

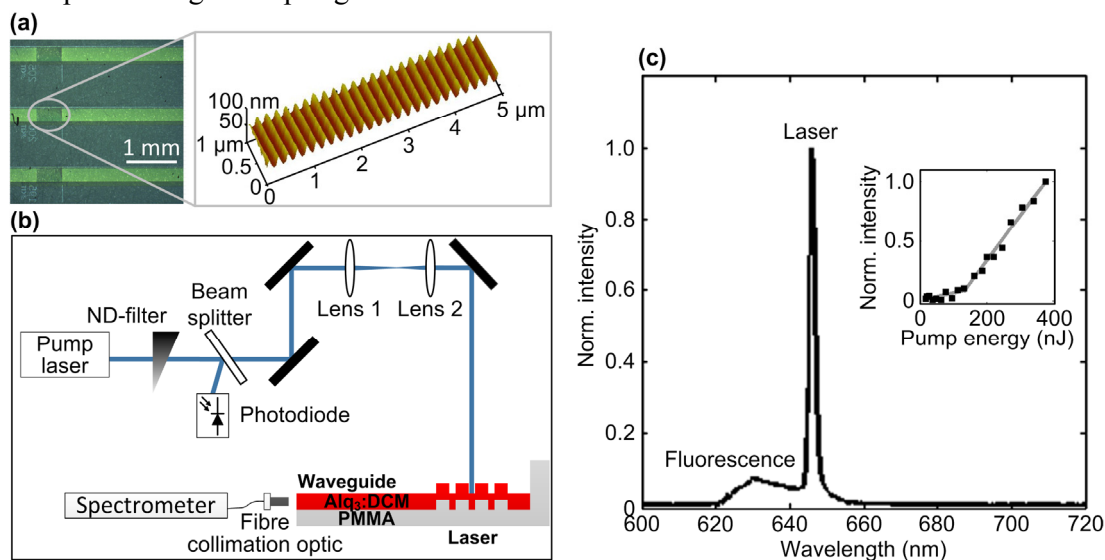


Fig. 4 (a) Microscope image of a coupled organic DFB edge-emitting laser (left) and an atomic force micrograph of the nanograting with period of $\Lambda = 200$ nm (right). (b) Schematic illustration of the optical setup to detect the edge emission from the integrated organic DFB laser. (c) Laser spectrum and input-output curve (inset) taken from the chip facet of grating $\Lambda = 200$ nm using a multimode optical fiber coupled to a spectrometer.

The experimental setup for the chip characterization is schematically depicted in Fig. 4(b). The pump laser and the detection system were the same as used for the characterization of the surface-emitting organic lasers, but we changed the detection plane according to the chip orientation. The excitation spot diameter on the sample surface was ~ 100 μm. In order to limit laser degradation in the ambient atmosphere, we set the excitation repetition rate as low as 100 Hz. Figure 4(c) shows exemplarily the laser spectrum of a DFB laser with a grating period of $\Lambda = 200$ nm. The laser emission at $\lambda = 645.5$ nm was detected at the chip facet using a multimode optical fiber (Ocean Optics, P400-3-UV-VIS). A stronger background due to the Alq₃:DCM fluorescence than in the case of the surface-emitting lasers is observed. This can be explained by the fact that the fluorescence is coupled into the waveguide with comparable efficiency as the laser radiation. In case of surface-emitting lasers the fluorescence is almost not detected as it is emitted into all directions. The corresponding laser threshold was measured to be 145 nJ/pulse. This higher

threshold can be explained with the laser being pumped at a larger excitation spot size than for the surface-emitting lasers.

4 Size-dependence of laser-assisted replication

The minimum replication area size is determined by the applied laser beam diameter, the used processing time, and the laser-induced heating temperature in the contact zone of master stamp and polymer. To investigate the spatial resolution limits of the replication process, we fabricated test structures with a tool comprising spatially defined DFB grating areas via laser-assisted replication using different heating periods. Figure 5(a) shows a microscope image of the beginning trail of the replicated structure, which was obtained by laser-induced heating of a single line with a scanning speed of 40 mm/s, corresponding to a ~ 17.5 ms-long local heating. The red line indicates a fit to the right end of the replicated structures. The rim is in good accordance with the elliptical laser focus spot size of $0.55 \text{ mm} \times 0.7 \text{ mm}$.

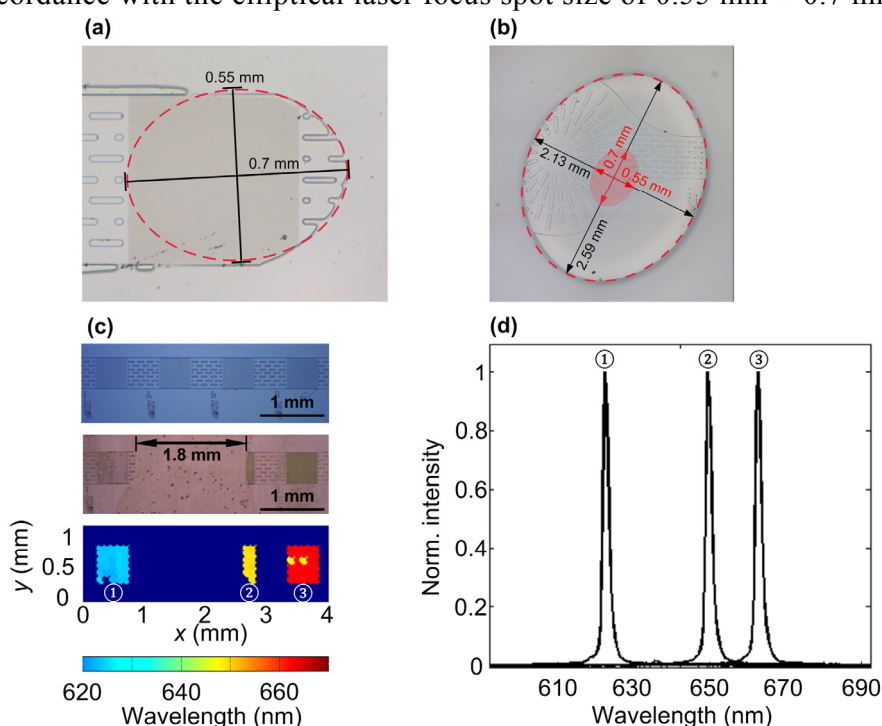


Fig. 5 Microscope images of (a) the begin of the replication trail obtained by heating a single line with a laser scanning velocity of 40 mm/s and (b) the replicated spot after 2 s-long punctuate heating in comparison with the laser focus spot (red). (c) Photograph of the complete set of spatially defined laser gratings (from left to right: $\Lambda = 390 \text{ nm}$, $\Lambda = 400 \text{ nm}$, $\Lambda = 410 \text{ nm}$ and $\Lambda = 420 \text{ nm}$) on silicon master stamp (top). The actual laser grating areas are visible as homogenous darker grey areas which are separated by auxiliary structures in between. The photograph of the PMMA laser pixels partially replicated on a PMMA chip (middle) and spatially resolved laser wavelengths of fabricated organic DFB laser pixels (bottom) are also shown. (d) Laser spectra corresponding to the grating areas ①, ② and ③ in (c).

In comparison, applying 2 s-long punctuate heating resulted in an expansion of the heat-affected zone on the silicon stamp and a consequently enlarged replication area. As shown in Fig. 5(b), an extension was measured as ~ 3.8 times of the laser focus spot size.

We verified the versatility of the localized replication by fabrication of preselected laser pixels. Figure 5(c) shows a partial replication from the silicon master stamp with gratings in periods of $\Lambda = 390 \text{ nm}$, $\Lambda = 400 \text{ nm}$, $\Lambda = 410 \text{ nm}$ and $\Lambda = 420 \text{ nm}$. Each pixel has a dimension of $500 \mu\text{m} \times 500 \mu\text{m}$ with an interspacing

of 500 μm . A 2 mm-broad space was excluded from the laser writing path from left to right on chip. As a result, we observed an unformed gap with a width of 1.8 mm between the replicated structures. The slightly smaller unstructured area is attributed to the heat conduction in the silicon master stamp. The spatially resolved lasing wavelength distribution revealed one completely omitted and one only partially available laser pixel. The latter had a clearly defined border. The corresponding laser pixel spectra are shown in Fig. 5(d).

As previously mentioned, a great advantage of the localized replication is the subsequent fabrication of nanostructures with already existing photonic, fluidic or electronic components, which remain unaffected during fabrication process. We demonstrated this by replicating the same structures twice on a single 2 mm-thick PMMA substrate and performing two successive replication processes at a distance of 10 mm. Each replicated area was defined to be $5 \times 20 \text{ mm}^2$ without overlapping each other, as shown in Fig. 6(a). Figure 6(b) shows a photograph of the finished laser pixels on PMMA chip, which can be clearly identified by the interference effect. A 250 nm-thick Alq_3 :DCM layer was evaporated on top of the chip to check the laser behavior and determine the replication quality. All laser pixels showed homogeneous laser emissions throughout the whole pixel area with corresponding wavelengths according to their DFB grating periods. Laser pixels having the same grating period revealed comparable characteristics, e.g., the laser thresholds of the laser pixels with grating period of $\Lambda = 420 \text{ nm}$ were measured to be 17.3 nJ/pulse and 14.8 nJ/pulse, both emitting at the same laser peak wavelength of $\lambda = 670 \text{ nm}$. The existing grating structures were not influenced by the subsequent replication process. This can be widely useful for LOC and other integrated optics applications. Inexpensive fabrication of identical nanostructures without repetitive construction on a master stamp is shown to be possible.

5 Encapsulation via laser transmission welding

During operation, organic semiconductors suffer from photoluminescence degradation when exposed to air or water. Therefore, an encapsulation is necessary to sustain a long lifetime of the device. Earlier, LOCs containing organic semiconductor lasers were encapsulated in polymer using thermal bonding,^{12,13} which is usually time-consuming and therefore only suitable for parallel processing with large numbers of LOC chips. In addition, high temperature used for bonding leads to bleaching of the organic dyes. Here, we demonstrate the encapsulation of our fabricated organic laser chip via laser transmission welding.³³ For this purpose, the same setup as for laser-assisted replication was used, as shown in Fig. 1. A 2 mm-thick PMMA substrate was prepared as a lid and placed on top of the previously fabricated chip with laser-pixel basins. Since PMMA is transparent for near-infrared radiation, an additional absorption layer of carbon with a thickness of 5-10 nm was deposited under the polymer chip, where the welding process was to be performed (chip edge). Applying the diode laser beam at a wavelength of $\lambda = 940 \text{ nm}$ on the chip edge with 5 mm-wide margin, the absorption layer converted the laser radiation into heat, which melted the two PMMA substrates along the contact area and bond them together (heating temperature, $T = 140 \text{ }^\circ\text{C}$; laser scan velocity, $v = 40 \text{ mm/s}$; clamping pressure, $p = 0.4 \text{ MPa}$; hatch distance, $\Delta x = 300 \text{ }\mu\text{m}$). A photograph of the encapsulated organic laser chip is shown in Fig. 6(c). As expected, the encapsulation process was found not to affect the emission

properties of the laser pixels. Laser transmission welding is thus not only a practical tool for chip bonding direct after laser-assisted replication, but also can be a substitute of thermal bonding after thermal nanoimprint lithography process.

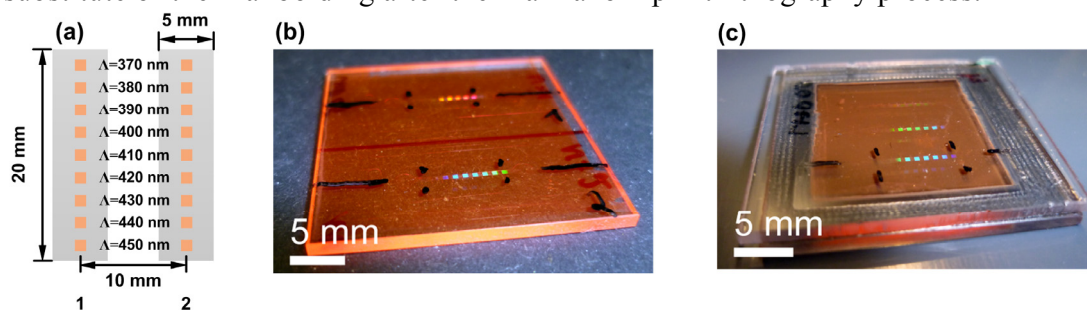


Fig. 6 (a) Scheme of the first and second laser-assisted replication area in size of 5 mm × 20 mm. (b) Photograph of subsequently fabricated grating structures 1 and 2. (c) Finished chip after encapsulation with PMMA lid via laser transmission welding. The chip edge looks silver due to the absorption layer of carbon.

6 Conclusion

In summary, we have successfully applied laser-assisted replication in fabrication of spatially localized organic semiconductor DFB laser pixels on PMMA chips. We accomplished nine surface-emitting laser pixels based on nanogratings with different periods in lateral dimension of $500\ \mu\text{m} \times 500\ \mu\text{m}$ on a PMMA substrate. We also realized a simultaneous fabrication of nanoscale DFB corrugations and neighboring microscale waveguide basins. After evaporation of the same active material, coupled edge-emitting organic lasers were achieved with combination of the functional waveguides. The minimum fabrication area size was investigated by comparing the replication spot with laser beam focus size and the versatility of spatially localized replication was verified by fabrication of preselected laser pixels. We also proved that using this fabrication method, further nanostructures could be added into the chip platform without negative influence on neighboring photonic components. Consequently, laser-assisted replication is an ideal tool for the fast and flexible fabrication of micro- and nanostructures with high quality, especially suited for rapid prototyping of LOC platforms. Finally, we completed the chip fabrication by encapsulation the polymeric chip using laser transmission welding. This progress in additive fabrication of grating can ideally be combined with our recent progress in ink-jet printing the active gain medium of organic semiconductors. By using different laser pixels, this approach allows for the realization of digitally manufactured versatile coherent light sources integrated in photonic microsystems and LOC devices.

Acknowledgments

The authors thank A. Bacher, P.-J. Jakobs and A. Muslija for silicon master stamp fabrication and P. Abaffy for taking scanning electron microscope images. This work was supported by the Deutsche Forschungsgemeinschaft and the State of Baden-Württemberg through the DFG-Center for Functional Nanostructures (CFN). The work of X. L. is supported by Carl Zeiss Stiftung and Karlsruhe School of Optics & Photonics (KSOP). We acknowledge support by Deutsche Forschungsgemeinschaft and Open Access Publishing Fund of Karlsruhe Institute of Technology. Finally, the support for laser processing by the Karlsruhe Nano Micro Facility (KNMF,

<http://www.knmf.kit.edu>) a Helmholtz research infrastructure at the Karlsruhe Institute of Technology is gratefully acknowledged.

References

- 1 N. Tessler, G. J. Denton and R. H. Friend, Lasing from conjugated-polymer microcavities, *Nature*, 1996, **382**, 695–697.
- 2 F. Hide, M. A. DiazGarcia, B. J. Schwartz, M. R. Andersson, Q. B. Pei and A. J. Heeger, Semiconducting polymers: A new class of solid-state laser materials, *Science*, 1996, **273**, 1833–1836.
- 3 S. V. Frolov, M. Ozaki, W. Gellermann, Z. V. Vardeny and K. Yoshino, Mirrorless lasing in conducting polymer poly(2,5-dioctyloxy-p-phenylenevinylene) films, *Jpn. J. Appl. Phys.*, 1996, **35**, L1371–L1373.
- 4 I. D. W. Samuel and G. A. Turnbull, Organic semiconductor lasers, *Chem. Rev.*, 2007, **107**, 1272–1295.
- 5 S. Klinkhammer, X. Liu, K. Huska, Y. Shen, S. Vanderheiden, S. Valouch, C. Vannahme, S. Bräse, T. Mappes and U. Lemmer, Continuously tunable solution-processed organic semiconductor DFB lasers pumped by laser diode, *Opt. Express*, 2012, **20**, 6357–6364.
- 6 Y. Oki, S. Miyamoto, M. Maeda and N. J. Vasa, Multiwavelength distributed-feedback dye laser array and its application to spectroscopy, *Opt. Lett.*, 2002, **27**, 1220–1222.
- 7 T. Woggon, S. Klinkhammer and U. Lemmer, Compact spectroscopy system based on tunable organic semiconductor lasers, *Appl. Phys. B*, 2010, **99**, 47–51.
- 8 S. Klinkhammer, T. Woggon, C. Vannahme, T. Mappes and U. Lemmer, Optical spectroscopy with organic semiconductor lasers, *Proc. SPIE*, 2010, **7722**, 77221I.
- 9 X. Liu, P. Stefanou, B. Wang, T. Woggon, T. Mappes and U. Lemmer, Organic semiconductor distributed feedback (DFB) laser as excitation source in Raman spectroscopy, *Opt. Express*, 2013, **21**, 28941–28947.
- 10 T. Mappes, C. Vannahme, M. Schelb, U. Lemmer and J. Mohr, Design for optimized coupling of organic semiconductor laser light into polymer waveguides for highly integrated bio-photonic sensors, *Microelectron. Eng.*, 2009, **86**, 1499–1501.
- 11 C. Vannahme, S. Klinkhammer, A. Kolew, P.-J. Jakobs, M. Guttmann, S. Dehm, U. Lemmer and T. Mappes, Integration of organic semiconductor lasers and single-mode passive waveguides into a PMMA substrate, *Microelectron. Eng.*, 2010, **87**, 693–695.
- 12 C. Vannahme, M. B. Christiansen, T. Mappes and A. Kristensen, Optofluidic dye laser in a foil, *Opt. Express*, 2010, **18**, 9280–9285.
- 13 C. Vannahme, S. Klinkhammer, M. B. Christiansen, A. Kolew, A. Kristensen, U. Lemmer and T. Mappes, All-polymer organic semiconductor laser chips: Parallel fabrication and encapsulation, *Opt. Express*, 2010, **18**, 24881–24887.
- 14 C. Vannahme, S. Klinkhammer, U. Lemmer and T. Mappes, Plastic lab-on-a-chip for fluorescence excitation with integrated organic semiconductor lasers, *Opt. Express*, 2011, **19**, 8179–8186.
- 15 H. Sirringhaus, T. Kawase, R. H. Friend, T. Shimoda, M. Inbasekaran, W. Wu and E. P. Woo, High-resolution inkjet printing of all-polymer transistor circuits, *Science*, 2000, **290**, 2123–2126.
- 16 H. E. Katz, Recent advances in semiconductor performance and printing processes for organic transistor-based electronics, *Chem. Mater.*, 2004, **16**, 4748–4756.
- 17 C. N. Hoth, P. Schilinsky, S. A. Choulis and C. J. Brabec, Printing highly efficient organic solar cells, *Nano Lett.*, 2008, **8**, 2806–2813.
- 18 T. Aernouts, T. Aleksandrov, C. Giroto, J. Genoe and J. Poortmans, Polymer based organic solar cells using ink-jet printed active layers, *Appl. Phys. Lett.*, 2008, **92**, 033306.
- 19 T. R. Hebner, C. C. Wu, D. Marcy, M. H. Lu and J. C. Sturm, Ink-jet printing of doped polymers for organic light emitting devices, *Appl. Phys. Lett.*, 1998, **72**, 519–521.
- 20 J. Bharathan and Y. Yang, Polymer electroluminescent devices processed by inkjet printing: I. Polymer light-emitting logo, *Appl. Phys. Lett.*, 1998, **72**, 2660–2662.
- 21 X. Liu, S. Klinkhammer, K. Sudau, N. Mechau, C. Vannahme, J. Kaschke, T. Mappes, M. Wegener and U. Lemmer, Ink-jet-printed organic semiconductor distributed feedback laser, *Appl. Phys. Express*, 2012, **5**, 072101.

- 22 X. Liu, S. Klinkhammer, Z. Wang, T. Wienhold, C. Vannahme, P.-J. Jakobs, A. Bacher, A. Muslija, T. Mappes and U. Lemmer, Pump spot size dependent lasing threshold in organic semiconductor DFB lasers fabricated via nanograting transfer, *Opt. Express*, 2013, **21**, 27697–27706.
- 5 23 R. Stabile, A. Camposeo and L. Persano, Organic-based distributed feedback lasers by direct electron-beam lithography on conjugated polymers, *Appl. Phys. Lett.*, 2007, **91**, 101110.
- 24 M. Stroisch, T. Woggon, U. Lemmer, G. Bastian, G. Violakis and S. Pissadakis, Organic semiconductor distributed feedback laser fabricated by direct laser interference ablation, *Opt. Express*, 2007, **15**, 3968–3973.
- 10 25 N. R. Hendricks and K. R. Carter, Nanoimprint lithography of polymers, in *Polymer Science: A Comprehensive Reference* (Elsevier, 2012), pp. 251–274.
- 26 S. Y. Chou, P. R. Krauss and P. J. Renstrom, Nanoimprint lithography, *J. Vac. Sci. Technol. B*, 1996, **14**, 4129–4133.
- 27 D. Pisignano, L. Persano, P. Visconti, R. Cingolani, G. Gigli, G. Barbarella and L. Favaretto, 15 Oligomer-based organic distributed feedback lasers by room-temperature nanoimprint lithography, *Appl. Phys. Lett.*, 2003, **83**, 2545–2547.
- 28 E. B. Namdas, M. Tong, P. Ledochowitsch, S. R. Mednick, J. D. Yuen, D. Moses and A. J. Heeger, Low thresholds in polymer lasers on conductive substrates by distributed feedback nanoimprinting: progress toward electrically pumped plastic lasers, *Adv. Mater.*, 2009, **21**, 20 799–802.
- 29 C. Ge, M. Lu, X. Jian, Y. Tan and B. T. Cunningham, Large-area organic distributed feedback laser fabricated by nanoreplica molding and horizontal dipping, *Opt. Express*, 2010, **18**, 12980–12991.
- 30 Y. Wang, G. Tsiminis, A. L. Kanibolotsky, P. J. Skabara, I. D.W. Samuel and G. A. Turnbull, 25 Nanoimprinted polymer lasers with threshold below 100 W/cm² using mixed-order distributed feedback resonators, *Opt. Express*, 2013, **21**, 14362–14367.
- 31 V. Grigaliunas, S. Tamulevicius, R. Tomasiunas, V. Kopustinskas, A. Guobiene and D. Jucius, Laser pulse assisted nanoimprint lithography, *Thin Solid Films*, 2004, **453**, 13–15.
- 32 V. Grigaliunas, S. Tamulevicius, M. Muehlberger, D. Jucius, A. Guobiene, V. Kopustinskas 30 and A. Gudonyte, Nanoimprint lithography using IR laser irradiation, *Appl. Surf. Sci.*, 2006, **253**, 646–650.
- 33 W. Pfleging, O. Baldus and A. Baldini, Method for joining plastic workpieces, European Patent No. EP20050739878 (27. Nov. 2013).
- 34 W. Pfleging, R. Kohler, I. Südmeyer and M. Rohde, Laser micro and nano processing of 35 metals, ceramics, and polymers, in *Laser-Assisted Fabrication of Materials*, J. D. Majumdar and I. Manna, eds. (Springer, 2013), pp. 319–374.
- 35 A. Singh, W. Pfleging, M. Beiser and C. K. Malek, Transparent thin thermoplastic biochip by injection-moulding and laser transmission welding, *Microsyst. Technol.*, 2013, **19**, 445–453.
- 36 X. Cheng and L. Jay Guo, One-step lithography for various size patterns with a hybrid mask- 40 mold, *Microelectron. Eng.*, 2004, **71**, 288–293.